Keihan Astrophysics Meeting 2024 fall

Parametric Instability of Fast Radio Burst in Magnetar Magnetosphere

Rei Nishiura

Division of Physics and Astronomy, Kyoto University

Shoma Kamijima; Masanori Iwamoto; Kunihito Ioka

Yukawa Institute for Theoretical Physics, Kyoto University

Outline

1. **Introduction**
2. Research contents
3. Discussion
4. Conclusion

What is a Fast Radio Burst (FRB) ?

FRBs are the brightest radio transients, first discovered in 2007. Lorimer et al. 2007

- Origin and mechanism of FRBs are not fully understood.
- **FRB 20200428 from the Galactic magnetar**

  marked a step

  towards understanding

  the phenomena.

  CHIME/FRB et al. 2020,
  Bochenek et al. 2020

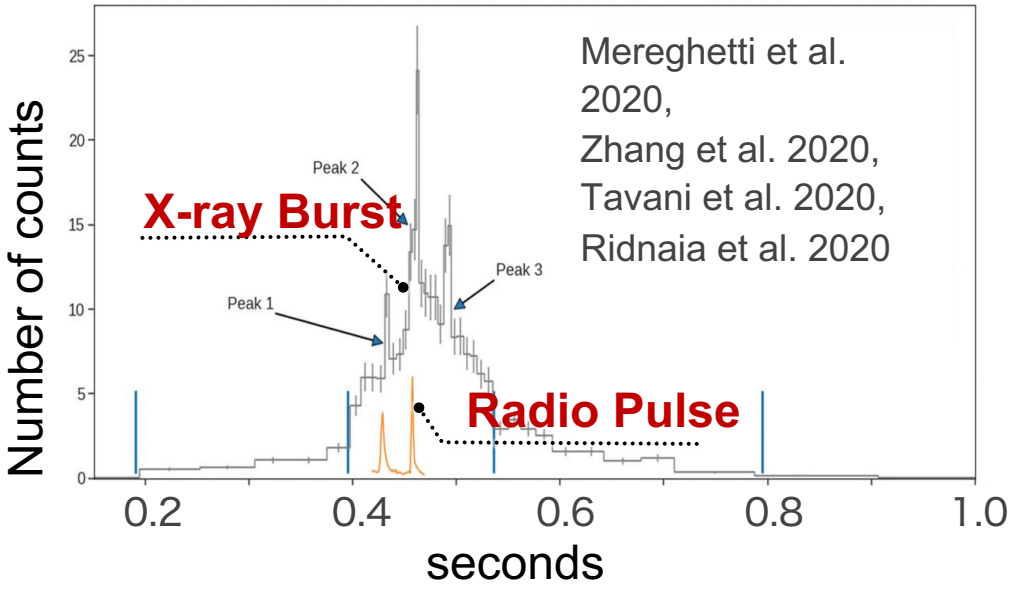

We want to clarify the FRB emission in magnetar.

FRB Emission Models in Magnetars

Two major locations for FRB generation in the magnetar are considered.

Magnetosphere models

Katz 2014; Lyutikov et al. 2016; Lu and Kumar 2018; Yang and Zhang 2018; Kumar and Bošnjak 2020; Cooper and Wijers 2021

Far-away models

Lyubarsky 2014; Murase et al. 2016; Waxman 2017; Margalit et al. 2020; Beloborodov 2020

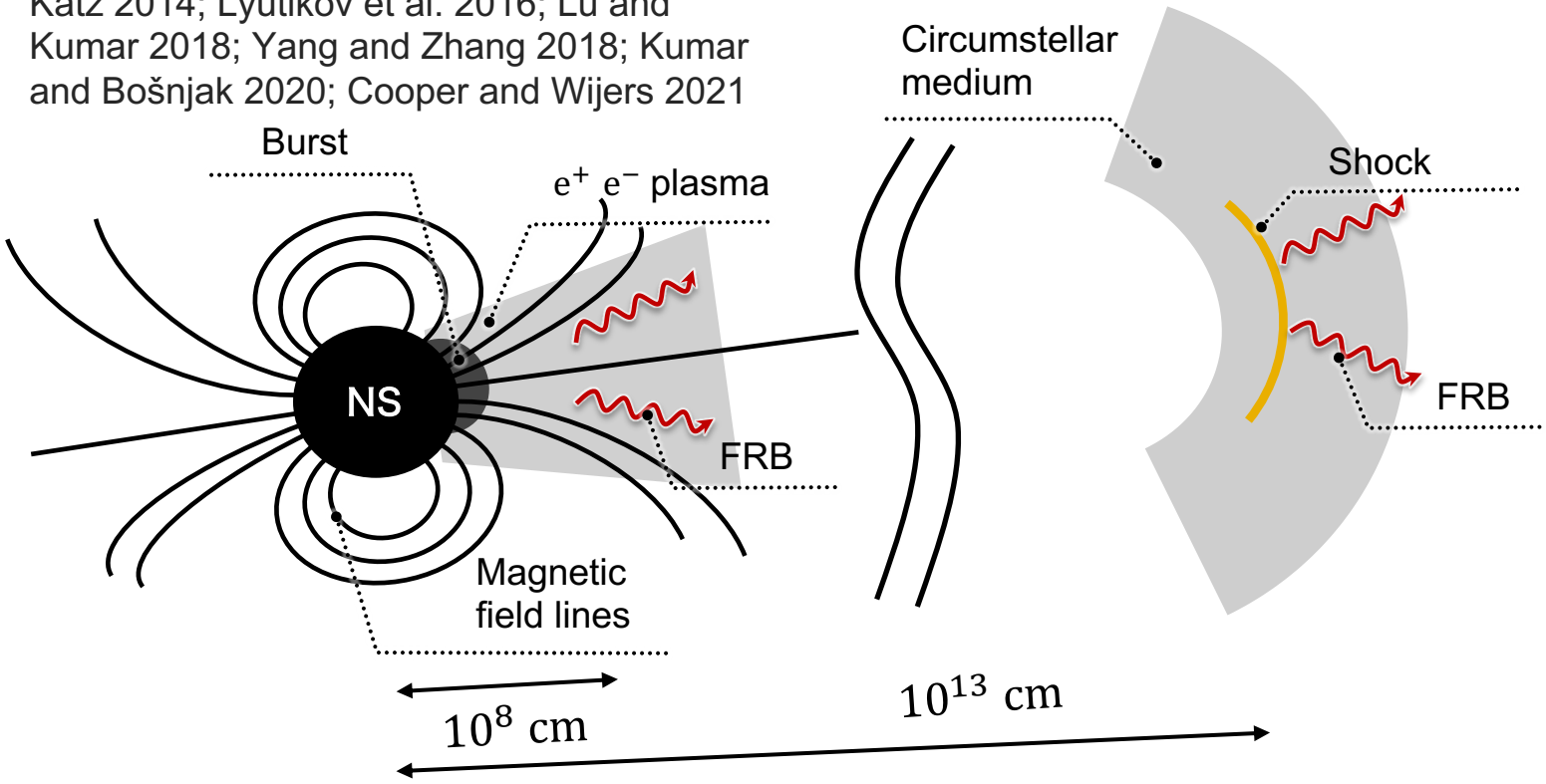

Scattering of FRBs in the Magnetosphere Model

Coherent waves (FRBs) can be significantly attenuated by induced Compton scattering in a magnetar magnetosphere.

Blandford and Scharlemann 1975; Wilson and Rees 1978; Wilson 1982; Lyubarskii and Petrova 1996; Lyubarsky 2008

$$t_{\rm dyn}^{-1} = \frac{c}{r} \sim 3.0\times10^{2}\ {\rm s}^{-1}\ r_8^{-1}$$

$$t_{\rm C}^{-1} \sim \frac{\omega_{\rm p}^2 a_{\rm e}^2}{\omega_0}$$

Lyubarsky 2021

Linear growth rate of induced Compton scattering

$\mathcal{M}$: multiplicity

$$a_{\rm e} \equiv \frac{2eE}{m_{\rm e} c \omega_0}$$

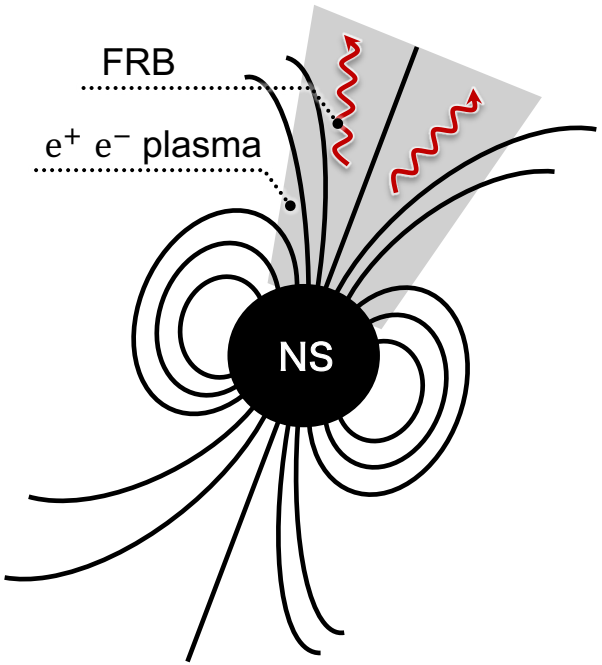

$$\sim 1.1\times10^{20}\ {\rm s}^{-1}\ \frac{B_{\rm p,14}\mathcal{M}_6 L_{38} R_{\rm NS,6}^3}{P_{\rm sec} r_8^5 \nu_9^3} \gg t_{\rm dyn}^{-1}$$

Parametric Instability

The beat between the incident and scattered waves resonantly generates plasma density fluctuations.

- A variety of instabilities exist.
- Stimulated Brillioun scattering
  $(\omega = kc_s)$
- **Induced Compton scattering**
  (Landau resonance)

Step 1

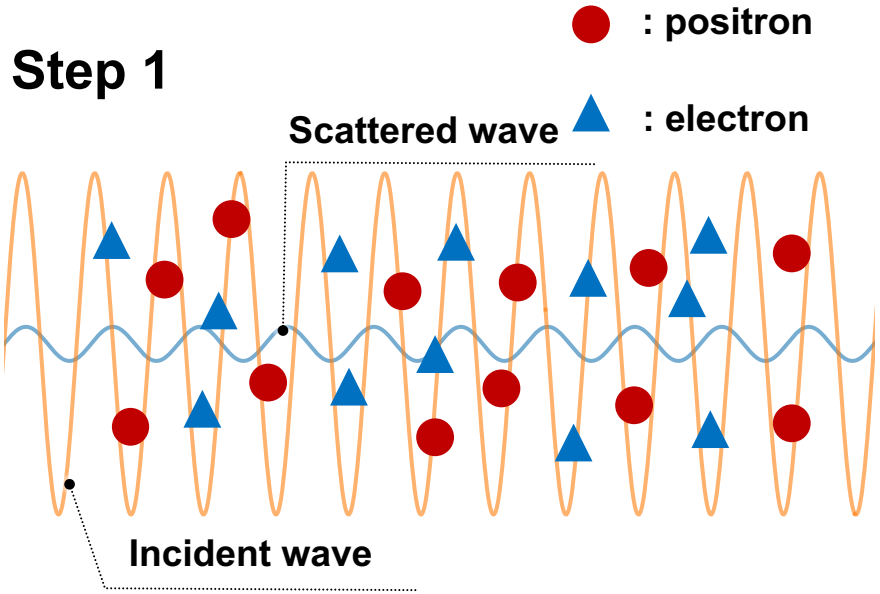

$$\omega_0 = \omega + \omega_1$$

Incident wave (Transverse wave) → Density fluctuation (Longitudinal wave) + Scattered wave (Transverse wave)

Parametric Instability

The beat between the incident and scattered waves resonantly generates plasma density fluctuations.

- A variety of instabilities exist.
- Stimulated Brillioun scattering
  $(\omega = kc_s)$
- **Induced Compton scattering**
  (Landau resonance)

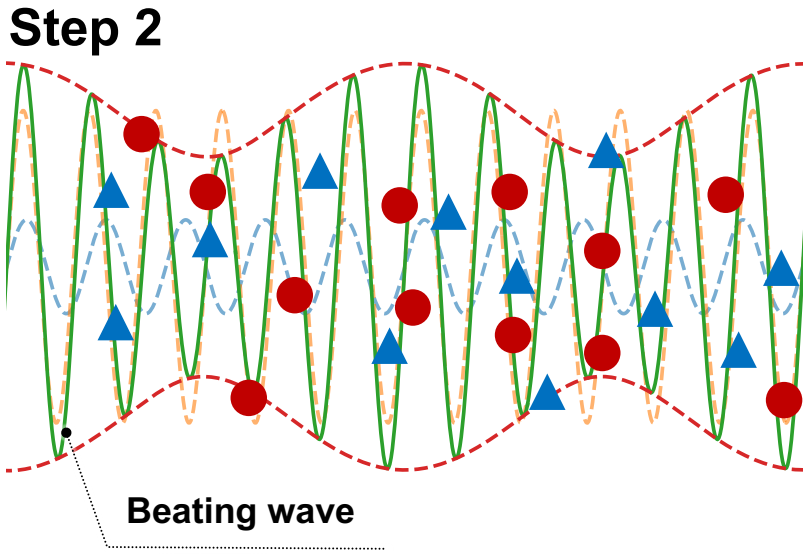

$\omega_0 = \omega + \omega_1$

Incident wave (Transverse wave) → Density fluctuation (Longitudinal wave) + Scattered wave (Transverse wave)

Ponderomotive Force (No background magnetic fields)

Charged particles experience a force toward regions of lower amplitude in a slowly varying field.

$$m_e \ddot{\boldsymbol{r}}_{0\pm} = -\nabla \phi_p$$

Oscillation center

$$\phi_p = \frac{e^2}{m_e \omega_0^2} \left\langle \frac{\left|E(\boldsymbol{r}_{0\pm}, t)\right|^2}{2} \right\rangle_{\text{time}}$$

Ponderomotive potential

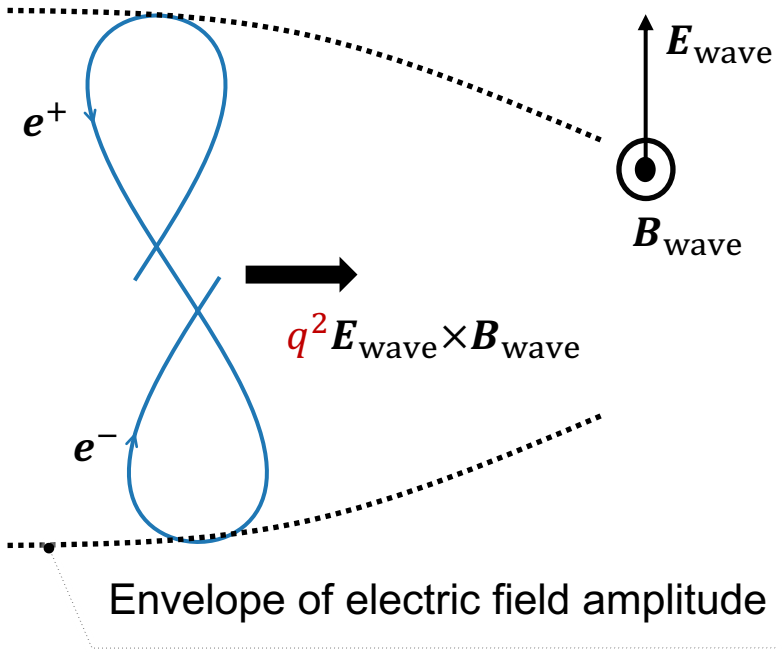

- The ponderomotive force does **NOT** depend on the charge sign in nonmagnetized plasma.

Parametric Instability

The beat between the incident and scattered waves resonantly generates plasma density fluctuations.

- A variety of instabilities exist.
- Stimulated Brillioun scattering
  $(\omega = kc_s)$
- **Induced Compton scattering**
  (Landau resonance)

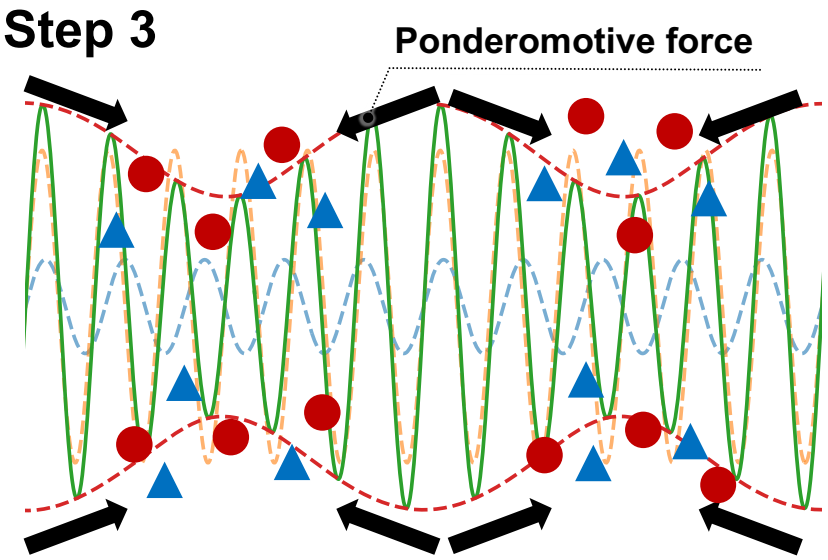

$\omega_0 = \omega + \omega_1$

Incident wave (Transverse wave) $\rightarrow$ Density fluctuation (Longitudinal wave) + Scattered wave (Transverse wave)

Suppression Effects in Scattering Cross-Section

In a strongly magnetized $e^{\pm}$ plasma, scattering of perpendicular polarized wave is greatly suppressed.

Canuto et al. 1971; Herold 1979; Ventura 1979; Meszaros 1992

$$\sigma_{\rm X} \sim \sigma_{\rm T} \left(\frac{\omega_0}{\omega_{\rm c}}\right)^2 \quad \text{for } \omega_{\rm c} \gg \omega_0$$

$$\omega_{\rm c} \equiv \frac{eB_0}{m_{\rm e}c}$$

$$t_{\rm C}^{-1} \sim \left(\frac{\omega_0}{\omega_{\rm c}}\right)^2 \frac{\omega_{\rm p}^2 a_{\rm e}^2}{\omega_0}$$

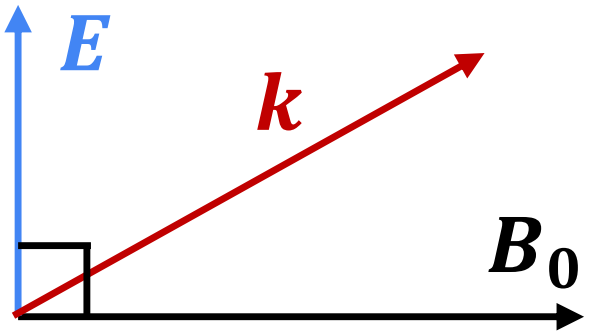

Blandford and Scharlemann 1976; Kumar and Lu 2020;

RN and Ioka 2024

$$\sim 4.5\times10^{8}\ {\rm s}^{-1}\ \frac{r_8 L_{38} \mathcal{M}_6 R_{\rm NS,6}^3}{B_{\rm p,14} \nu_9 P_{\rm sec}} \gg t_{\rm dyn}^{-1} \sim 3.0\times10^{2}\ {\rm s}^{-1}$$

Does induced Compton scattering have the same suppression factor?

Outline

1. Introduction
2. **Research contents**
3. Discussion
4. Conclusion

Vlasov equation for $e^{\pm}$ plasma

Drake et al. (1974)：nonmagnetized ion-electron plasma

Our study：**magnetized** electron-**positron** plasma

$$\frac{\partial f_{\pm}}{\partial t} + \boldsymbol{v} \cdot \frac{\partial f_{\pm}}{\partial \boldsymbol{r}} + \boldsymbol{F} \cdot \frac{\partial f_{\pm}}{\partial \boldsymbol{p}} = 0$$

$$\boldsymbol{F} = \underbrace{\pm e\left(\boldsymbol{E} + \frac{\boldsymbol{v}\times\boldsymbol{B}_0}{c}\right)}_{\text{Lorentz force exerted on the plasma}} \underbrace{- \nabla\phi_{\pm}}_{\text{Ponderomotive force in a magnetic field}}$$

The new terms we introduce in this study

$$\nabla \cdot \boldsymbol{E} = 4\pi\rho = \sum_{q=\pm e} 4\pi q n_{\mathrm{e}0} \int \mathrm{d}^3\boldsymbol{v}\, \delta f_{\pm}$$: Maxwell equation

$$f_{\pm}(\boldsymbol{r}, \boldsymbol{v}, t) = f_{0\pm}(\boldsymbol{v}) + \delta f_{\pm}(\boldsymbol{r}, \boldsymbol{v}, t)$$

How to derive the linear growth timescale?

We take the imaginary part of the dispersion relation for scattered wave.

$$(c^2k_1^2 - \omega_1^2)A_1 = 4\pi c \frac{\boldsymbol{A}_1}{A_1} \cdot \tilde{\boldsymbol{J}} \qquad \text{: Dispersion relation}$$

$$\tilde{\boldsymbol{J}}_{\text{nonlinear}} = e\widetilde{\delta n}_+ \boldsymbol{v}_{0+}^* - e\widetilde{\delta n}_- \boldsymbol{v}_{0-}^*$$

$$\widetilde{\delta n}_\pm = n_{\text{e}0} \int \mathrm{d}^3\boldsymbol{v}\, \widetilde{\delta f}_\pm \qquad \delta f(\boldsymbol{r},\boldsymbol{v},t) \equiv \mathrm{e}^{i(\boldsymbol{k}\cdot\boldsymbol{r}-\omega t)}\widetilde{\delta f}(\boldsymbol{k},\boldsymbol{v},\omega) + \text{c. c.}$$

$$= -\frac{n_{\text{e}0}}{m_{\text{e}}}\left\{\widetilde{\phi_\pm}\sum_{l=-\infty}^{+\infty}\int \mathrm{d}^3\boldsymbol{v}\, \frac{J_l^2(k_\perp r_{\text{L}\pm})\boldsymbol{k}\cdot\frac{\partial f_0}{\partial \boldsymbol{v}^*}}{\omega - k_\parallel v_\parallel \mp l\omega_{\text{c}}}\right\}$$

$$\pm\frac{n_{\text{e}0}H_\pm}{m_{\text{e}}\varepsilon_{\text{L}}}\left\{\widetilde{\phi_+}\sum_{l=-\infty}^{+\infty}\int \mathrm{d}^3\boldsymbol{v}\, \frac{J_l^2(k_\perp r_{\text{L}+})\boldsymbol{k}\cdot\frac{\partial f_0}{\partial \boldsymbol{v}^*}}{\omega - k_\parallel v_\parallel - l\omega_{\text{c}}} - \widetilde{\phi_-}\sum_{l=-\infty}^{+\infty}\int \mathrm{d}^3\boldsymbol{v}\, \frac{J_l^2(k_\perp r_{\text{L}-})\boldsymbol{k}\cdot\frac{\partial f_0}{\partial \boldsymbol{v}^*}}{\omega - k_\parallel v_\parallel + l\omega_{\text{c}}}\right\}$$

The linear growth timescale for the scattered wave

There are two types of induced Compton scattering, and a new suppression factor is obtained.

$$t_{\mathrm{C}}^{-1} = \sqrt{\frac{\pi}{32\mathrm{e}}} \underbrace{\left(\frac{\omega_0}{\omega_{\mathrm{c}}}\right)^2}_{\text{Magnetic effects}} \frac{\omega_{\mathrm{p}}^2 a_{\mathrm{e}}^2}{\omega_0} \frac{m_{\mathrm{e}} c^2}{k_{\mathrm{B}} T_{\mathrm{e}}}$$

$$\frac{8 k_{\mathrm{B}} T_{\mathrm{e}}}{m_{\mathrm{e}} c^2} \left(\frac{\omega_0}{\omega_{\mathrm{p}}}\right)^2 \geq 1$$

The previously considered growth timescale

$$t_{\mathrm{C}}^{-1} = \sqrt{\frac{\pi}{32\mathrm{e}}} \underbrace{\left(\frac{\omega_0}{\omega_{\mathrm{c}}}\right)^2}_{\text{Magnetic effects}} \frac{\omega_{\mathrm{p}}^2 a_{\mathrm{e}}^2}{\omega_0} \frac{m_{\mathrm{e}} c^2}{k_{\mathrm{B}} T_{\mathrm{e}}}$$

$$\frac{8 k_{\mathrm{B}} T_{\mathrm{e}}}{m_{\mathrm{e}} c^2} \left(\frac{\omega_0}{\omega_{\mathrm{p}}}\right)^2 \ll 1$$

$$\times \max\left\{ \underbrace{\frac{32\mathrm{e}}{\pi} \left(\frac{\omega_0}{\omega_{\mathrm{p}}}\right)^4 \left(\frac{k_{\mathrm{B}} T_{\mathrm{e}}}{m_{\mathrm{e}} c^2}\right)^2}_{\text{Charged mode}}, \underbrace{\left(\frac{\omega_0}{\omega_{\mathrm{c}}}\right)^2}_{\text{Neutral mode}} \right\}$$

New suppression factor !

Outline

1. Introduction
2. Research contents
3. **Discussion**
4. Conclusion

Induced Compton scattering with Debye screening

Induced Compton scattering of the charged mode is suppressed by Debye screening.

$$t_{\mathrm{charged}}^{-1} = \sqrt{\frac{\pi}{32\mathrm{e}}}\left(\frac{\omega_0}{\omega_\mathrm{c}}\right)^2 \frac{\omega_\mathrm{p}^2 a_\mathrm{e}^2}{\omega_0}\frac{m_\mathrm{e}c^2}{k_\mathrm{B}T_\mathrm{e}} \times \underbrace{\frac{32\mathrm{e}}{\pi}\left(\frac{\omega_0}{\omega_\mathrm{p}}\right)^4 \left(\frac{k_\mathrm{B}T_\mathrm{e}}{m_\mathrm{e}c^2}\right)^2}_{\wr\ \left(\frac{\lambda_\mathrm{Debye}}{\lambda_0}\right)^2} \qquad \left(\frac{\lambda_\mathrm{Debye}}{\lambda_0}\right)^2 \ll 1$$

$$\lambda_\mathrm{Debye} \equiv \left(\frac{k_\mathrm{B}T_\mathrm{e}}{8\pi e^2 n_\mathrm{e}}\right)^{\frac{1}{2}}$$

λ_0 : Wavelength of the incident wave

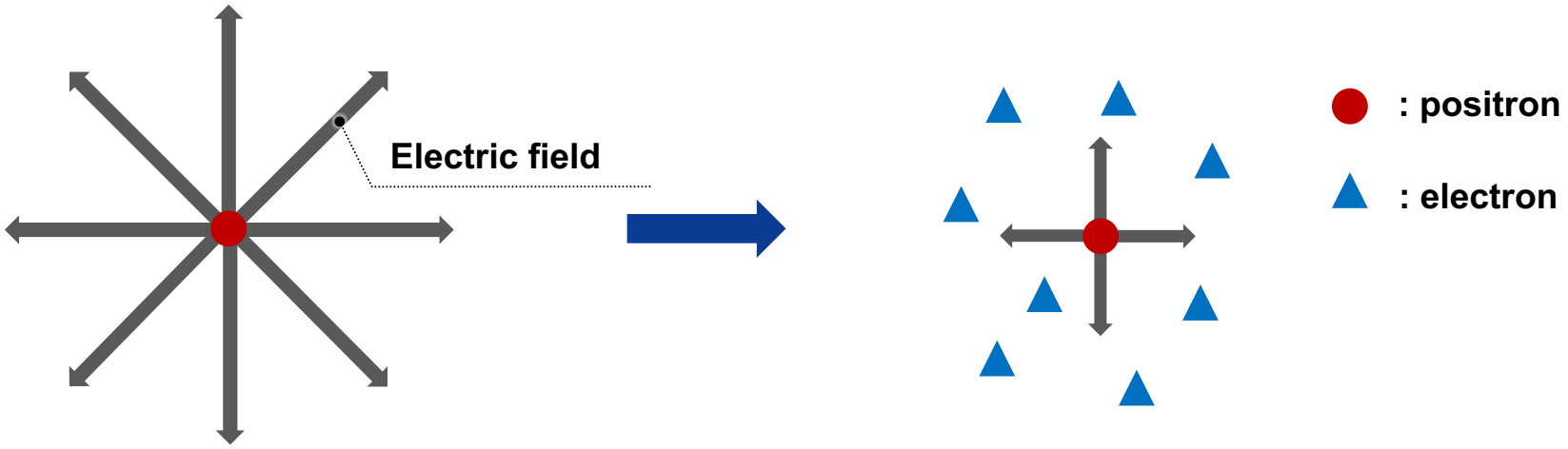

Ponderomotive force in a magnetic field

The ponderomotive force induces charge separation in strongly magnetized $e^{\pm}$ plasma.

Cary and Kaufman 1977; Hatori and Washimi 1981; Lee and Parks 1983; Lee and Parks 1996

$$\phi_{\pm} = \frac{e^2}{2m_{\mathrm{e}}}\left\langle \frac{E_{\parallel}^2}{\omega_0^2} - \frac{E_{\perp}^2}{\omega_{\mathrm{c}}^2 - \omega_0^2} \pm i\frac{\omega_{\mathrm{c}}\left(E_z^* E_y - E_y^* E_z\right)}{\omega_0(\omega_{\mathrm{c}}^2 - \omega_0^2)} \right\rangle$$

Charged mode $\sim \mathcal{O}(\omega_0/\omega_{\mathrm{c}})$

● : positron

▲ : electron

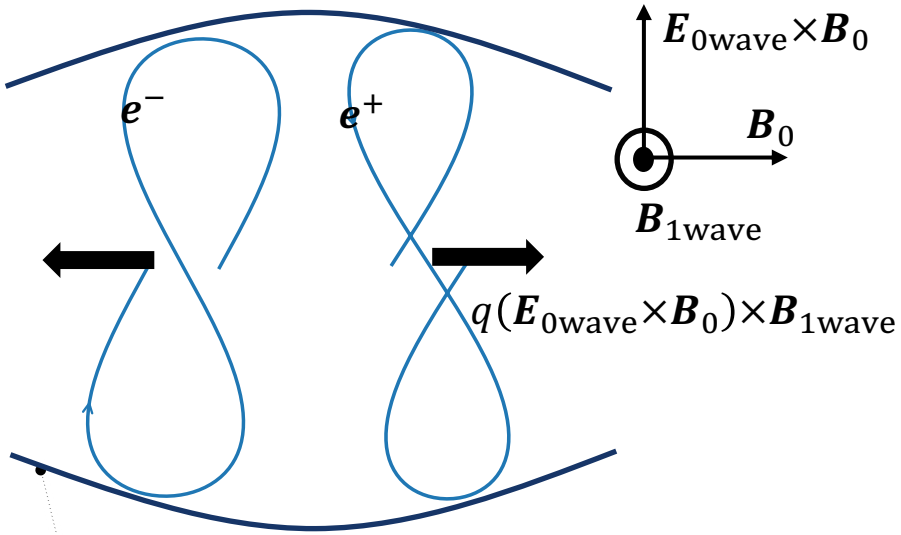

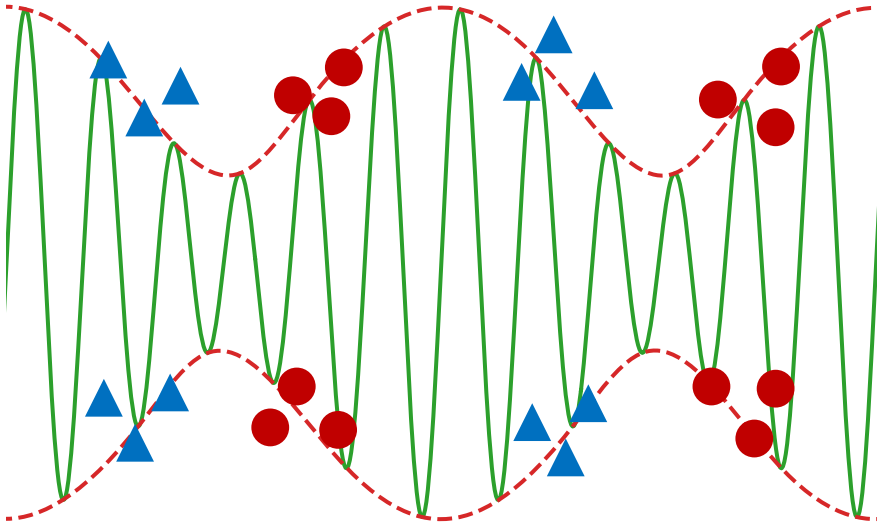

Envelope of electric field amplitude

The order estimation for FRBs from magnetosphere

FRBs can propagate even in the mangetar magnetosphere of the large plasma density.

$$t_{\rm dyn}^{-1} \sim 3.0\times10^{2}\ {\rm s}^{-1}\ r_8^{-1}$$

$$t_{\rm charged}^{-1} \sim 9.3\times10^{2}\ {\rm s}^{-1}\ \frac{P_{\rm sec} r_8^7 L_{38} T_{80{\rm keV}}^2}{\nu_9^2 B_{\rm p,14}^3 \mathcal{M}_6 R_{\rm NS,6}^9} \sim t_{\rm dyn}^{-1}$$

$$t_{\rm neutral}^{-1} \sim 1.8\times10^{-2}\ {\rm s}^{-1}\ \frac{r_8^7 \nu_9 L_{38} \mathcal{M}_6}{B_{\rm p,14}^3 P_{\rm sec} R_{\rm NS,6}^9} \ll t_{\rm dyn}^{-1}$$

c.f. $t_{\rm old}^{-1} \sim 4.5\times10^{8}\ {\rm s}^{-1}\ \frac{r_8 L_{38} \mathcal{M}_6 R_{\rm NS,6}^3}{B_{\rm p,14} \nu_9 P_{\rm sec}} \gg t_{\rm dyn}^{-1}$

Previous studies have overestimated the reaction rate.

Outline

1. Introduction
2. Research contents
3. Discussion
4. **Conclusion**

Conclusion

We formulated induced Compton scattering in a background magnetic field for the first time.

- Both the magnetic field and Debye screening are important in strongly magnetized $e^{\pm}$ plasma.

$$t_{\mathrm{C}}^{-1} = \sqrt{\frac{\pi}{32\mathrm{e}}}\left(\frac{\omega_0}{\omega_{\mathrm{c}}}\right)^2 \frac{\omega_{\mathrm{p}}^2 a_{\mathrm{e}}^2}{\omega_0}\frac{m_{\mathrm{e}}c^2}{k_{\mathrm{B}}T_{\mathrm{e}}} \qquad \frac{8k_{\mathrm{B}}T_{\mathrm{e}}}{m_{\mathrm{e}}c^2}\left(\frac{\omega_0}{\omega_{\mathrm{p}}}\right)^2 \ll 1$$

$$\times \max\left\{\underbrace{\frac{32\mathrm{e}}{\pi}\left(\frac{\omega_0}{\omega_{\mathrm{p}}}\right)^4\left(\frac{k_{\mathrm{B}}T_{\mathrm{e}}}{m_{\mathrm{e}}c^2}\right)^2}_{\text{Charged mode}}, \underbrace{\left(\frac{\omega_0}{\omega_{\mathrm{c}}}\right)^2}_{\text{Neutral mode}}\right\} \ll t_{\mathrm{C,old}}^{-1}$$

- **FRBs can sufficiently escape the magnetar magnetosphere** even if they undergo induced Compton scattering.

予備スライド

Mode Coupling

When one pendulum is oscillated, energy is transferred through the spring to the other pendulum.

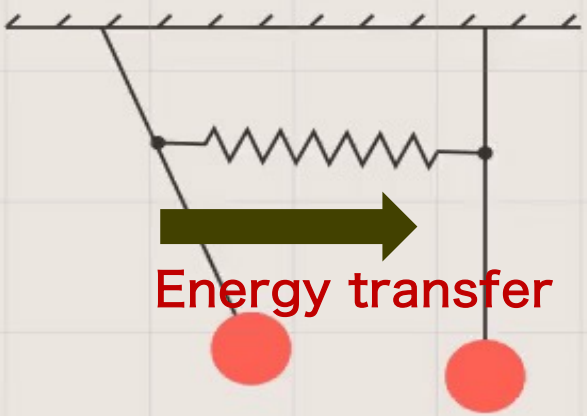

Left pendulum (Transverse wave) → The spring oscillation (Longitudinal wave) + Right pendulum (Transverse wave)

パラメトリック不安定 (うなり電磁波の生成)

プラズマに電磁波が入射すると、散乱波とうなりを生じる

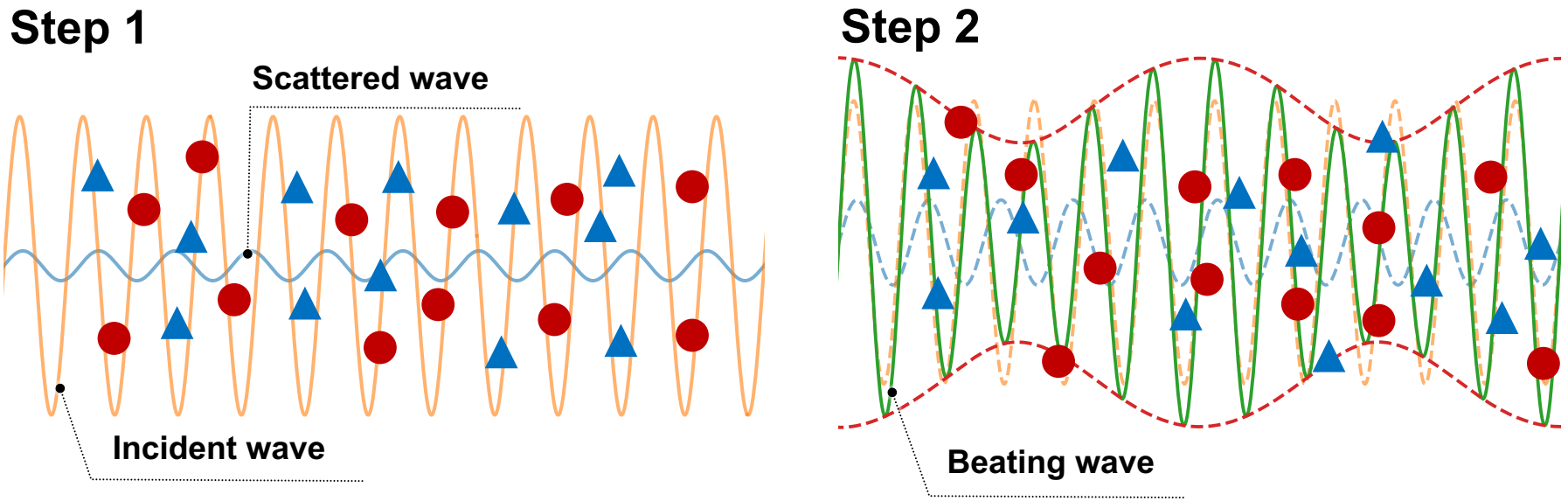

- 散乱波は、background wave あるいは熱的粒子からのトムソン散乱で生じる

ポンデロモーティブ力 (背景磁場無し)

振幅がゆっくり変動する電磁波中で、荷電粒子は
振幅の小さい方向に力を受ける

$$m_{\mathrm{e}}\ddot{\boldsymbol{r}}_{0\pm} = -\nabla\phi_{\mathrm{p}}$$

粒子の振動中心

$$\phi_{\mathrm{p}} = \frac{e^2}{m_{\mathrm{e}}\omega_0^2}\left\langle\frac{\left|E(\boldsymbol{r}_{0\pm},t)\right|^2}{2}\right\rangle_{\mathrm{time}}$$

Ponderomotive potential

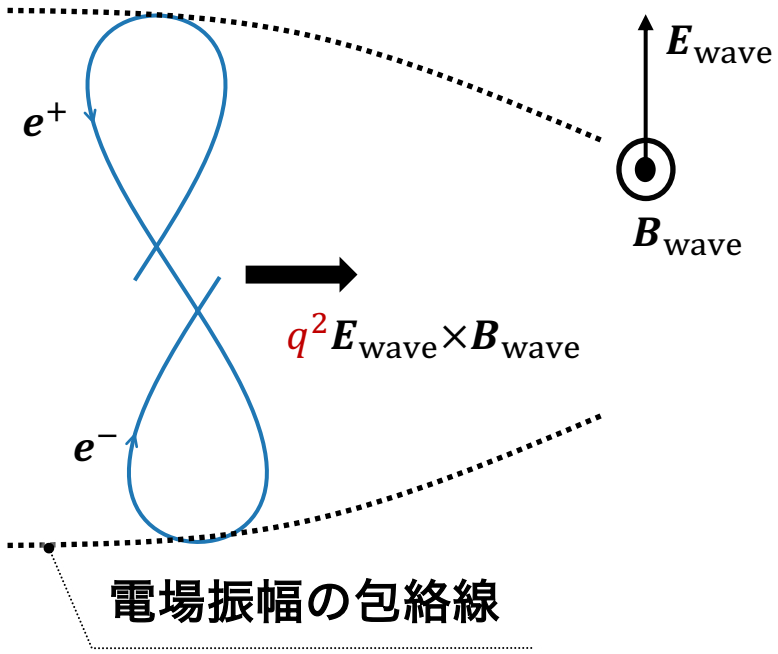

- ポンデロモーティブ力は電荷符号に依存しない **(磁場無し)**

パラメトリック不安定 (密度ゆらぎの生成)

荷電粒子が振幅の小さい方にポンデロモーティブ力を受け密度揺らぎが生じる

- 様々なパラメトリック不安定が存在する
  - 誘導ブリルアン散乱 $(\omega = kc_s)$
  - 誘導ラマン散乱 $(\omega = \omega_p)$

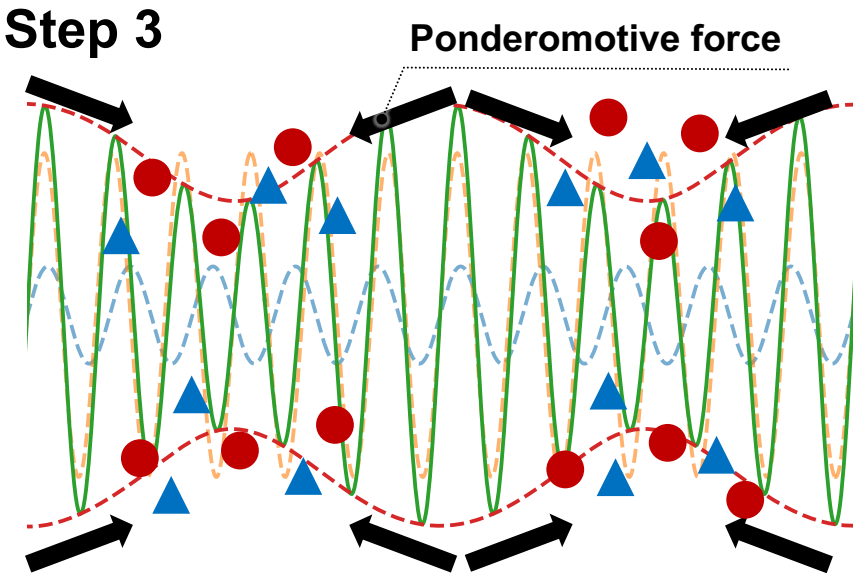

$\omega_0 = \omega + \omega_1$

入射電磁波 (横波) → 密度揺らぎ (縦波) + 散乱電磁波 (横波)

c.f. 振り子 (横波) → ばね振動 (縦波) + 振り子 (横波)

(非線形)ランダウ減衰と誘導コンプトン散乱

誘導コンプトン散乱は、うなりの位相速度と同程度で運動する粒子とのランダウ減衰で記述される

- 通常のランダウ減衰：**波の位相速度**程度で運動する粒子が波からエネルギーをもらう
- 誘導コンプトン散乱：**うなりの位相速度**程度で運動する粒子が波からエネルギーをもらって電磁波が減衰

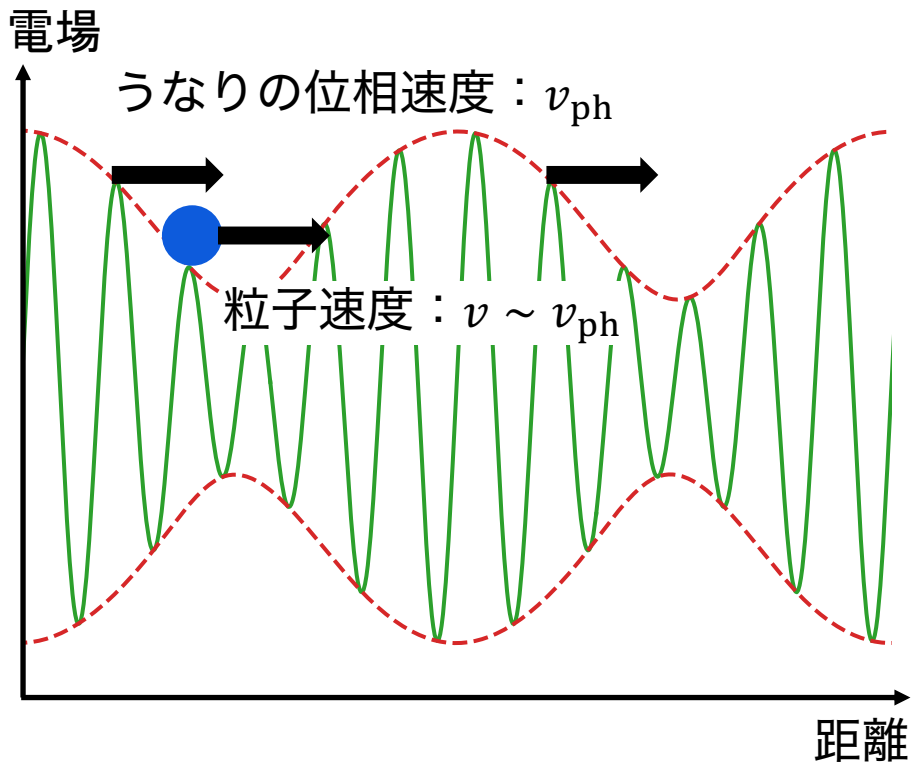

背景磁場中のうなり波で作られる密度揺らぎ

密度揺らぎが電流を生成し、これが波動方程式のソース項に加わることで不安定を引き起こす

$$\delta\widetilde{n}_{\pm} = n_{\mathrm{e}0}\int \mathrm{d}^3\boldsymbol{v}\,\delta\widetilde{f}_{\pm}$$

$$= -\frac{n_{\mathrm{e}0}}{m_{\mathrm{e}}}\left\{\widetilde{\phi}_{\pm}\sum_{l=-\infty}^{+\infty}\int \mathrm{d}^3\boldsymbol{v}\,\frac{J_l^2(k_\perp r_{\mathrm{L}\pm})\boldsymbol{k}\cdot\dfrac{\partial f_0}{\partial \boldsymbol{v}^*}}{\omega - k_\parallel v_\parallel \mp l\omega_{\mathrm{c}}}\right\}$$

$$\pm\frac{n_{\mathrm{e}0}H_{\pm}}{m_{\mathrm{e}}\varepsilon_{\mathrm{L}}}\left\{\widetilde{\phi}_{+}\sum_{l=-\infty}^{+\infty}\int \mathrm{d}^3\boldsymbol{v}\,\frac{J_l^2(k_\perp r_{\mathrm{L}+})\boldsymbol{k}\cdot\dfrac{\partial f_0}{\partial \boldsymbol{v}^*}}{\omega - k_\parallel v_\parallel - l\omega_{\mathrm{c}}} - \widetilde{\phi}_{-}\sum_{l=-\infty}^{+\infty}\int \mathrm{d}^3\boldsymbol{v}\,\frac{J_l^2(k_\perp r_{\mathrm{L}-})\boldsymbol{k}\cdot\dfrac{\partial f_0}{\partial \boldsymbol{v}^*}}{\omega - k_\parallel v_\parallel + l\omega_{\mathrm{c}}}\right\}$$

$$\delta f(\boldsymbol{r},\boldsymbol{v},t) \equiv \mathrm{e}^{i(\boldsymbol{k}\cdot\boldsymbol{r}-\omega t)}\widetilde{\delta f}(\boldsymbol{k},\boldsymbol{v},\omega) + \mathrm{c.c.}$$

H: 縦電気感受率

ε_{L}: 縦誘電率

$$\tilde{\boldsymbol{j}}_{\mathrm{nonlinear}} = e\delta\widetilde{n}_{+}\boldsymbol{v}^*_{0+} - e\delta\widetilde{n}_{-}\boldsymbol{v}^*_{0-}$$

電子・陽電子が入射電磁波で揺らされる運動

$$\boldsymbol{k}\cdot\frac{\partial f_0}{\partial \boldsymbol{v}^*} \equiv k_\parallel\frac{\partial f_{0\pm}}{\partial v_\parallel} \pm \frac{l\omega_{\mathrm{c}}}{v_\perp}\frac{\partial f_{0\pm}}{\partial v_\perp}$$

$$r_{\mathrm{L}\pm} \equiv \pm\frac{v_\perp}{\omega_{\mathrm{c}}}$$

磁場中のポンデロモーティブ力：neutral mode

電荷分離を引き起こさないポンデロモーティブ力は非支配的

Cary and Kaufman 1977; Hatori and Washimi 1981; Lee and Parks 1983; Lee and Parks 1996

$$\phi_{\pm} = \frac{e^2}{2m_e}\left\langle \frac{E_{\parallel}^2}{\omega_0^2} - \frac{E_{\perp}^2}{\omega_c^2 - \omega_0^2} \pm i\,\frac{\omega_c\left(E_z^* E_y - E_y^* E_z\right)}{\omega_0(\omega_c^2 - \omega_0^2)} \right\rangle$$

Neutral mode $\sim \mathcal{O}(\omega_0/\omega_c)^2 \quad \omega_0 \ll \omega_c$

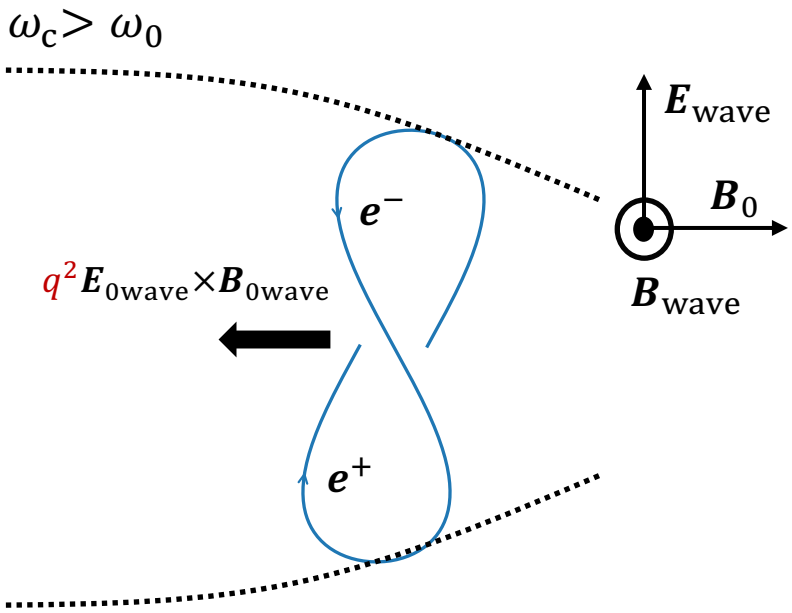

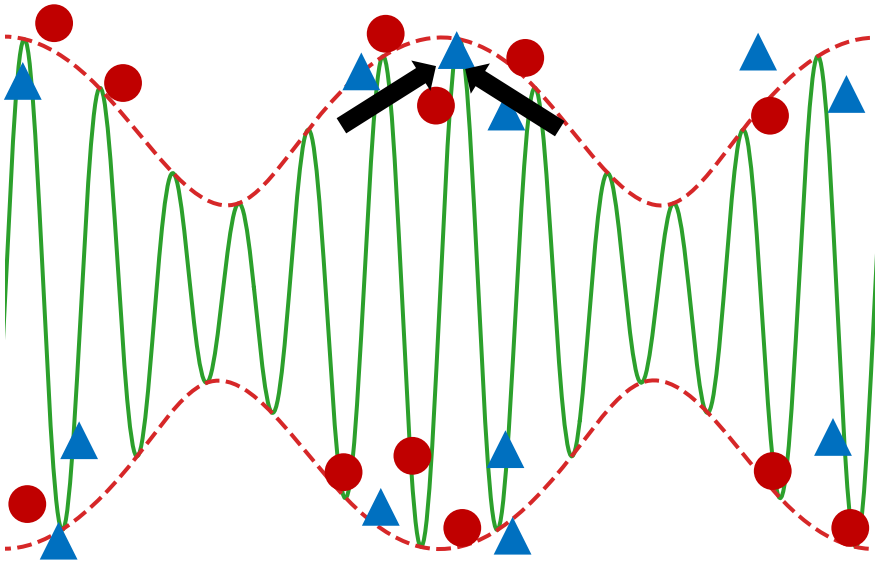

Narrowband or wideband FRBs

Broadband FRB に対する誘導コンプトン散乱も考える必要がある

Pleunis et al. 2021

- FRB の~30%は

  broadband spectrum (図左)

  $\Delta\nu/\nu \sim 1$

  Galactic FRB 20200428
  はこちらに分類される

- FRB の~60% は

  narrowband spectrum (図右)

  $\Delta\nu/\nu \ll 1$

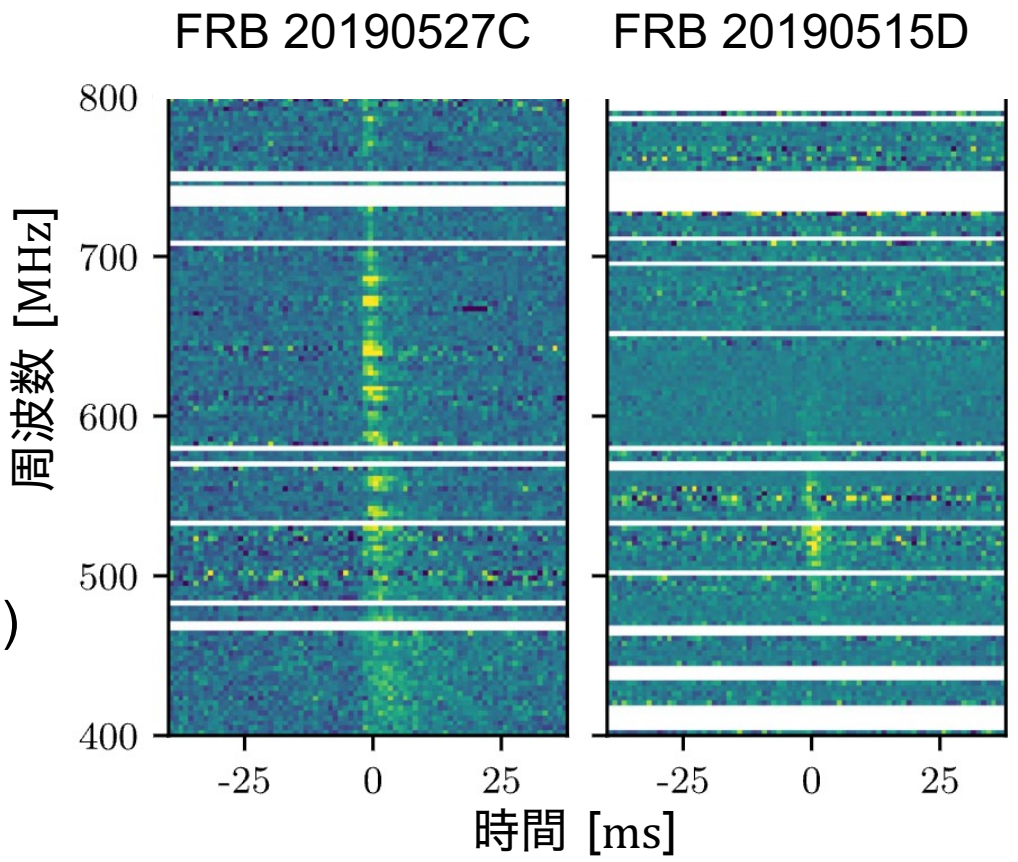

Broadband 入射波の場合のセットアップ

簡単のため入射波のみをbroadbandにする

$$\boldsymbol{A}(\boldsymbol{r},t)=\boldsymbol{A}_0\mathrm{e}^{\mathrm{i}(\boldsymbol{k}_0\cdot\boldsymbol{r}-\omega_0 t)}+\boldsymbol{A}_1\mathrm{e}^{\mathrm{i}(\boldsymbol{k}_1\cdot\boldsymbol{r}-\omega_1 t)}+\mathrm{c.c.}$$

$$\boldsymbol{A}(\boldsymbol{r},t)=\int\frac{\mathrm{d}\omega_0'}{2\pi}\boldsymbol{A}_0\mathrm{e}^{\mathrm{i}(\boldsymbol{k}_0\cdot\boldsymbol{r}-\omega_0' t)}+\boldsymbol{A}_1\mathrm{e}^{\mathrm{i}(\boldsymbol{k}_1\cdot\boldsymbol{r}-\omega_1 t)}+\mathrm{c.c.}$$

入射波　　散乱波

Broadband 入射波の場合のセットアップ

Broadband入射波の場合、反応率がさらに抑制される

Ghosh et al. 2022

$$t_{\rm charged}^{-1} = \sqrt{\frac{32{\rm e}}{\pi}} \frac{\omega_{\rm p}^2 a_{\rm e}^2}{\omega_0} \left(\frac{\omega_0}{\omega_{\rm c}}\right)^2 \left(\frac{\omega_0}{\omega_{\rm p}}\right)^4 \frac{k_{\rm B} T_{\rm e}}{m_{\rm e} c^2}$$

$$t_{\rm neutral}^{-1} = \sqrt{\frac{\pi}{32{\rm e}}} \left(\frac{\omega_0}{\omega_{\rm c}}\right)^4 \frac{\omega_{\rm p}^2 a_{\rm e}^2}{\omega_0} \left(\frac{k_{\rm B} T_{\rm e}}{m_{\rm e} c^2}\right)^{-1}$$

$$t_{\rm charged}^{\rm broad,-1} \sim \frac{\omega_{\rm p}^2 a_{\rm e}^2}{\omega_0} \left(\frac{\omega_0}{\omega_{\rm c}}\right)^2 \left(\frac{\omega_0}{\omega_{\rm p}}\right)^4 \left(\frac{k_{\rm B} T_{\rm e}}{m_{\rm e} c^2}\right)^{\frac{3}{2}}$$

$$t_{\rm neutral}^{\rm broad,-1} \sim \frac{\omega_{\rm p}^2 a_{\rm e}^2}{\omega_0} \left(\frac{\omega_0}{\omega_{\rm c}}\right)^4$$

予備スライド

Nonlinear current as functions of $\widetilde{\phi_\pm}$ and $\boldsymbol{v}_{0\pm}^{(1)}$

$$\widetilde{\boldsymbol{j}_1}^{*\mathrm{nonlinear}}(\boldsymbol{k}_1,\omega_1) = e\delta\widetilde{n}_+\,\boldsymbol{v}_{0+}^{(1)*} - e\delta\widetilde{n}_-\boldsymbol{v}_{0-}^{(1)*}$$

$$= (\cdots)\widetilde{\phi_+}\,\boldsymbol{v}_{0+}^{(1)*} + (\cdots)\widetilde{\phi_-}\,\boldsymbol{v}_{0+}^{(1)*} + (\cdots)\widetilde{\phi_-}\,\boldsymbol{v}_{0-}^{(1)*} + (\cdots)\widetilde{\phi_+}\,\boldsymbol{v}_{0-}^{(1)*}$$

$$\phi_\pm = \frac{e^2}{2m_\mathrm{e}}\left\langle\frac{E_\parallel^2}{\omega_0^2}\right\rangle - \frac{e^2}{2m_\mathrm{e}}\left\langle\frac{E_\perp^2}{\omega_\mathrm{c}^2-\omega_0^2}\right\rangle \pm \mathrm{i}\frac{e^2}{2m_\mathrm{e}}\left\langle\frac{\omega_\mathrm{c}\left(E_z^*E_y - E_y^*E_z\right)}{\omega_0(\omega_\mathrm{c}^2-\omega_0^2)}\right\rangle$$

$$\boldsymbol{v}_{0\pm}^{(1)} = \mp\frac{e}{m_\mathrm{e}c}\boldsymbol{A}_{0\parallel} \mp \frac{e}{m_\mathrm{e}c}\frac{\omega_0^2}{\omega_0^2-\omega_\mathrm{c}^2}\boldsymbol{A}_{0\perp} - \mathrm{i}\frac{e}{m_\mathrm{e}c}\frac{\omega_0\omega_\mathrm{c}}{\omega_0^2-\omega_\mathrm{c}^2}\boldsymbol{A}_0\times\widehat{\boldsymbol{B}}_0$$

Excited mode		Neutral mode	Charged mode
Polarization of incident wave	Parallel	Perpendicular	Perpendicular
	$\boldsymbol{A}_{0\perp}=\boldsymbol{0}$	$\boldsymbol{A}_{0\parallel}=\boldsymbol{0}$	$\boldsymbol{A}_{0\parallel}=\boldsymbol{0}$

将来展望

- 強磁場下における他のパラメトリック不安定の線形成長率の導出

  誘導ブリルアン散乱、誘導ラマン散乱、フィラメント不安定、e.t.c.

$$\widetilde{\delta n_{\pm}} = n_{\mathrm{e}0} \int \mathrm{d}^3\boldsymbol{v}\, \widetilde{\delta f_{\pm}}$$

$$= -\frac{n_{\mathrm{e}0}}{m_{\mathrm{e}}} \left\{ \widetilde{\phi_{\pm}} \sum_{l=-\infty}^{+\infty} \int \mathrm{d}^3\boldsymbol{v}\, \frac{J_l^2(k_{\perp} r_{\mathrm{L}\pm})\boldsymbol{k} \cdot \frac{\partial f_0}{\partial \boldsymbol{v}^*}}{\omega - k_{\parallel} v_{\parallel} \mp l\omega_{\mathrm{c}}} \right\}$$

$$\pm \frac{n_{\mathrm{e}0} H_{\pm}}{m_{\mathrm{e}} \varepsilon_{\mathrm{L}}} \left\{ \widetilde{\phi_{+}} \sum_{l=-\infty}^{+\infty} \int \mathrm{d}^3\boldsymbol{v}\, \frac{J_l^2(k_{\perp} r_{\mathrm{L}+})\boldsymbol{k} \cdot \frac{\partial f_0}{\partial \boldsymbol{v}^*}}{\omega - k_{\parallel} v_{\parallel} - l\omega_{\mathrm{c}}} - \widetilde{\phi_{-}} \sum_{l=-\infty}^{+\infty} \int \mathrm{d}^3\boldsymbol{v}\, \frac{J_l^2(k_{\perp} r_{\mathrm{L}-})\boldsymbol{k} \cdot \frac{\partial f_0}{\partial \boldsymbol{v}^*}}{\omega - k_{\parallel} v_{\parallel} + l\omega_{\mathrm{c}}} \right\}$$

- 非線形成長段階や成長の飽和段階はどうなっているか？

➡ Particle-in-Cell (PIC) シミュレーションによる検証が必要

予備スライド

予備スライド

予備スライド